Conformational Dynamics of Bovine Cu, Zn Superoxide Dismutase Revealed by Time-Resolved Fluorescence Spectroscopy of the Single Tyrosine Residue

Sergio T. Ferreira, Lorenzo Stella, and Enrico Gratton

Laboratory for Fluorescence Dynamics, Department of Physics, University of Illinois at Urbana-Champaign, Urbana, Illinois 61801 USA

ABSTRACT   The structural dynamics of bovine erythrocyte Cu, Zn superoxide dismutase (BSOD) was studied by time-resolved fluorescence spectroscopy. BSOD is a homodimer containing a single tyrosine residue (and no tryptophan) per subunit. Frequency-domain fluorometry revealed a heterogeneous fluorescence decay that could be described with a Lorentzian distribution of lifetimes. The lifetime distribution parameters (center and width) were markedly dependent on temperature. The distribution center (average lifetime) displayed Arrhenius behavior with an E_a of 4.2 kcal/mol, in contrast with an E_a of 7.4 kcal/mol for the single-exponential decay of L-tyrosine. This indicated that thermal quenching of tyrosine emission was not solely responsible for the effect of temperature on the lifetimes of BSOD. The distribution width was broad (1 ns at 8°C) and decreased significantly at higher temperatures. Furthermore, the width of the lifetime distribution increased in parallel to increasing viscosity of the medium. The combined effects of temperature and viscosity on the fluorescence decay suggest the existence of multiple conformational substates in BSOD that interconvert during the excited-state lifetime. Denaturation of BSOD by guanidine hydrochloride produced an increase in the lifetime distribution width, indicating a larger number of conformations probed by the tyrosine residue in the denatured state. The rotational mobility of the tyrosine in BSOD was also investigated. Analysis of fluorescence anisotropy decay data enabled resolution of two rotational correlation times. One correlation time corresponded to a fast (picosecond) rotation that contributed 62% of the anisotropy decay and likely reported local mobility of the tyrosine ring. The longer correlation time was 50% of the expected value for rotation of the whole (dimeric) BSOD molecule and appeared to reflect segmental motions in the protein in addition to overall tumbling. Comparison between rotational correlation times and fluorescence lifetimes of BSOD indicates that the heterogeneity in lifetimes does not arise from mobility of the tyrosine per se, but rather from dynamics of the protein matrix surrounding this residue which affect its fluorescence decay.

INTRODUCTION

A considerable amount of evidence has accumulated on the dynamic nature of protein structures and on the connection between protein dynamics and function (for reviews, see Wuthrich, 1976; Gurd and Rothgeb, 1979; Careri et al., 1979; Karplus and McCammon, 1981; Frauenfelder and Gratton, 1986; Frauenfelder et al., 1988). Given this connection, the importance of investigating protein structural dynamics towards an understanding of the molecular and energetic basis of protein function can be clearly recognized. Small fluctuations of the protein structure about the mean conformation depend on the particular nature of the conformational landscape of the protein matrix, which gives rise to nearly isoenergetic conformations. The interconversion between different substates depends on the height of the energy barriers between substates and on temperature (Frauenfelder and Gratton, 1986). Protein interactions, protein substates, ligand

binding, and viscosity affect the conformational landscape, hence the protein conformational fluctuations.

Intrinsic fluorescence spectroscopy has found wide application in characterizing protein conformational changes, which is largely due to the sensitivity of tryptophan (trp) fluorescence to physicochemical characteristics of the environment. The fluorescence decay of trp in proteins is usually complex, and several exponential components may be required to describe the decay even for proteins containing a single trp residue (Beechem and Brand, 1985). To provide a physical interpretation for the heterogeneity of protein fluorescence in the framework of a large number of protein conformational substates, distributions of lifetime values have been introduced (Alcala et al., 1987a–c; Gratton et al., 1989; Libertini and Small, 1989). In this view, fluorescence lifetime distributions originate from the existence of multiple conformational substates of the protein, and distribution analysis of fluorescence decay data may provide information on the conformational landscape and enable detection of dynamics of the protein matrix on a picosecond/nanosecond time scale (Alcala et al., 1987a–c). The heterogeneity of the fluorescence decay (expressed as the width of the lifetime distribution) was shown to be related to microheterogeneity of trp environments arising from conformational dynamics of the protein (Alcala et al., 1987c; Gratton et al., 1988; Bismuto et al., 1988; Ferreira, 1989; Ferreira and Gratton, 1990; Rosato et al., 1990 a, b; Mei et al., 1992). All studies so far, however, have made use of tryptophan (trp) fluorescence. In proteins lacking trp it remained to be investigated whether

information on protein dynamics can also be obtained from the fluorescence emission of other intrinsic fluorophores, such as tyr residues. In addition, the local mobility of tyr residues is generally larger than that of trp residues, and the comparison between trp and tyr fluorescence in proteins can provide a better understanding of the role of the protein matrix or local differences in the orientation of the residue in determining the heterogeneity of the lifetimes. Complex fluorescence decays have been observed for a number of proteins containing a single tyr residue (see Ross et al., 1992 for a review). However, to date lifetime distributions have not been utilized to describe the fluorescence decay of tyr in proteins as a tool to study protein conformational dynamics.

Superoxide dismutases (SOD) are enzymes that catalyze the dismutation of the superoxide free radical, thereby participating in the cellular defense mechanisms against oxidative damage. SOD activity has been related to various pathophysiological conditions including reperfusion damage after ischemia, aging, and neurodegenerative disorders (Zweier et al., 1987; Rusting, 1992; McNamara and Fridovich, 1993; Rosen et al., 1993). Considerable interest is currently focused on the understanding of the structural basis of the changes in SOD function that may lead to pathogenesis (Deng et al., 1993). Bovine erythrocyte Cu, Zn superoxide dismutase (BSOD) is a homodimer containing a single solvent exposed tyr residue (tyr 108) per subunit (Tainer et al., 1982). In this work, we have used tyr-108 as an intrinsic probe to investigate the dynamics of BSOD. This work extends previous studies from this laboratory that indicated a correlation between fluorescence decay and dynamics of human Cu, Zn SOD, a homologous protein containing a single trp residue (and no tyr) (Rosato et al., 1990 a, b; Mei et al., 1992). We show that the fluorescence decay of BSOD is heterogeneous, and that the heterogeneity is markedly dependent on temperature, viscosity, and unfolding of the protein. These effects are interpreted in terms of changes in dynamics of the protein matrix. Fluorescence anisotropy decay measurements further indicated that the heterogeneity of the fluorescence decay originated from conformational dynamics of the protein matrix surrounding the tyr residue rather than from differences in the local orientation of the tyr residue. Comparison of the present results with those previously reported for human SOD shows considerable qualitative agreement, which indicates that the structural information obtained in both studies is related to the conformational dynamics of the protein and does not depend on the nature, photophysics, or position of the intrinsic fluorescence probe (tyr 108 in BSOD versus trp 32 in human SOD). This lends support to the conclusion that time-resolved fluorescence of intrinsic fluorophores may be effectively used as a probe of dynamic events of the protein matrix.

MATERIALS AND METHODS

Protein

BSOD was purchased from Fluka Chem. Corp. (Ronkonkoma, NY) and purified to homogeneity by anion-exchange chromatography (Bannister and

Bannister, 1984). Protein purity was confirmed by SDS-PAGE and aminoacid composition analysis. Aminoacid analysis was performed at the UIUC Biotechnology Center Facility; no measurable amount of contaminating trp was detected, further indicating the purity of BSOD preparations. Enzymatic activity of purified BSOD was assayed as described by Paoletti and Mocali (1990) and was ~24,000–30,000 IU/mg of protein. Protein concentration was determined at 280 nm (Bannister et al., 1971). Samples contained 60 μM BSOD in 10 mM Tris-HCl, pH 7.6, containing 1 mM DTT (included to prevent possible cysteine oxidation and formation of intersubunit disulfide cross-links). Visible spectrophotometry was used to determine the presence of metals (Cu and Zn) in the protein. Holo-SOD was used throughout this work. For denaturation experiments, GdHCl in powder was added to the protein solution; measurements were carried out at 20°C after incubation with the desired concentration of GdHCl for 20 h at 4°C.

Steady-state fluorescence measurements

These were performed on an ISS (ISS Inc., Champaign, IL) photon-counting spectrofluorometer at 22°C with 8-nm bandpass for both excitation and emission. Corrected excitation spectra were obtained using a quantum-counter rhodamine 6G solution before the reference photomultiplier. Spectra were corrected for background signal, which was always <1% of the total intensity.

Time-resolved fluorescence measurements

A frequency-domain fluorometer was used. Excitation at 283 nm was provided by a mode-locked Nd-YAG laser (Antares model, Coherent, Palo Alto, CA) used to pump a cavity-dumped, externally frequency-doubled Rhodamine 6G dye-laser (model 700, Coherent). Emission was collected through a UV-30 filter (Hoya) to remove any scattered light. Phase-modulation lifetime measurements were carried out at 12 frequencies from 7 to 220 MHz. Color errors due to photomultiplier response were minimized by the use of reference standard solutions of p-terphenyl (Eastman Kodak, Rochester, NY) in cyclohexane or ethanol (lifetime = 1.05 ns). All lifetime measurements were carried out at "magic angle" configuration. Temperature was controlled with a thermocouple placed in the thermostated sample holder. Time-resolved anisotropy decay measurements were performed in the same instrument by differential polarized phase fluorometry (Weber, 1977) at 14 frequencies from 7 to 220 MHz.

Data analysis

Phase-modulation data were analyzed with the Globals Unlimited software (Beechem et al., 1991). Data were analyzed with different models including one, two, or three exponential lifetimes, or continuous lifetime distributions of different shapes (see Results). Goodness of fit was assessed by the value of minimized χ^2, which was calculated using standard deviations of $\pm 0.2°$ and ± 0.004 for phase angles and modulation ratios, respectively. Rigorous χ^2-surface error analysis was performed to define the resolvability and evaluate uncertainties of the recovered fit parameters (Beechem and Gratton, 1988). Statistical evaluation and comparison between results obtained with different decay models employing different numbers of fitting parameters was carried out using F-statistics analysis (Motulsky and Ransnas, 1987).

Differential polarized phase data obtained at different temperatures were globally analyzed using the Globals Unlimited software by incorporating the independently measured parameters for the decay of the fluorescence intensity (Beechem et al., 1991). The anisotropy decay was assumed to originate from a single rotator possessing one or two independent rotational motions (i.e., single- or bi-exponential anisotropy decays, respectively) and whose fluorescence intensity decay was described by a Lorentzian lifetime distribution. Calculation of χ^2 for the fits employed standard deviations of $\pm 0.2°$ and ± 0.007 for differential phase angles and modulation ratios, respectively.

Materials

Ultrapure GdHCl was obtained from Schwartz/Mann Biotech. (Cleveland, OH) and was checked for purity by UV absorption and fluorescence spec-

troscopy. Ultra-pure glycerol (obtained from USB Corp. (Cleveland, OH) and re-destilled to remove traces of fluorescent impurities) was a kind gift of Dr. N. Silva (Mayo Clinic, Rochester, MN). All other reagents were of the highest analytical grade available.

RESULTS

Fluorescence emission and corrected excitation spectra of purified BSOD are shown in Fig. 1. The spectra are typical of tyrosine fluorescence, with maximal excitation at 283 nm and maximal emission at 306 nm. This indicates absence of any contaminating tryptophan emission. It is also noteworthy that the fluorescence excitation and absorption spectra differ significantly in the region below 270 nm (Fig. 1). The absence of fine structure in the excitation spectrum in this region indicates absence of resonance energy transfer from the phenylalanines of BSOD (4 residues per subunit) to tyr 108. Thus, the fluorescence emission of BSOD is exclusively attributable to tyr 108 and is not complicated by energy transfer effects.

Frequency-domain lifetime measurements of BSOD were performed in the temperature range from 8–45°C. Fig. 2 shows phase-shift and demodulation plots at three different temperatures for a typical experiment. Data were initially analyzed with one-, two-, or three-exponential fluorescence decay models (Table 1). Single-exponential analysis was inadequate to describe the fluorescence decay of BSOD at any temperature investigated, yielding high χ^2 values (Table 1). Use of a double-exponential model resulted in improvement in χ^2 values, and further decreases in χ^2 were obtained with the triple-exponential analysis (Table 1). The improvement obtained with the three-exponential analysis was caused by the existence of a minor, very short component (τ_3) with a

FIGURE 2 Phase-modulation plots for BSOD at different temperatures. Multi-frequency phase angle and modulation ratio measurements were performed for BSOD at different temperatures. Phase angles (+, $\triangle$, $\square$) and modulation ratios ($\times$, O, $\mathbb{X}$) are plotted as a function of modulation frequency for experiments at 8, 25, and 45°C, respectively. Solid lines correspond to Lorentzian distribution fits (see text).

lifetime ranging from below 10 (our estimated low-limit instrumental resolution) to 40 ps, and a fractional intensity ranging from 1 to 3% of the total fluorescence. These characteristics suggest that this component in the analysis is due to light scattering, and the improvement in χ^2 is possibly due to the ability to account for this small amount of parasitic light with the three-exponential model.

To be meaningful, fits of protein fluorescence decay data should not only give good mathematical fits to the data (i.e., low χ^2 values) but should also be able to provide a physical interpretation of the decay in terms of different protein conformations. The general assumption in a multi-exponential lifetime fit is that each exponential lifetime can be associated to a specific discrete conformation of the protein. If this assumption is true, then the effects of different conditions of the medium (e.g., temperature) on the individual lifetimes should follow some definite trend. In other words, each of the individual protein conformations (and hence its characteristic lifetime) could be affected or not by temperature, but one expects physical continuity in the observed effects. Examination of the temperature dependence of the lifetimes and fractional intensities recovered in the three-exponential analysis of BSOD data reveals that some of these parameters display a complex behavior as a function of temperature (Table 1): for example, τ_2 initially decreases from 8 to 15°C, increases from 15 to 26°C, and finally decreases again from 26 to 45°C; f_2 (the fractional intensity of τ_2) initially increases from 8 to 15°C, decreases from 15 to 30°C, increases again from 30 to 36°C, and finally decreases at 45°C. Similar complex behavior is observed with f_1, the fractional intensity of the major lifetime component τ_1. The same behavior was also observed in the two-exponential analysis (Table 1). Thus, it is difficult to assign the effects of temperature on each lifetime to effects on discrete protein conformations. These considerations suggest that, although the three-exponential analysis provided good mathematical fits to the data, interpretation of the results in terms of discrete protein conformations was not appropriate to explain the effects of temperature on BSOD.

An alternative interpretation for the results of a multi-exponential fit is that the recovered parameters represent a
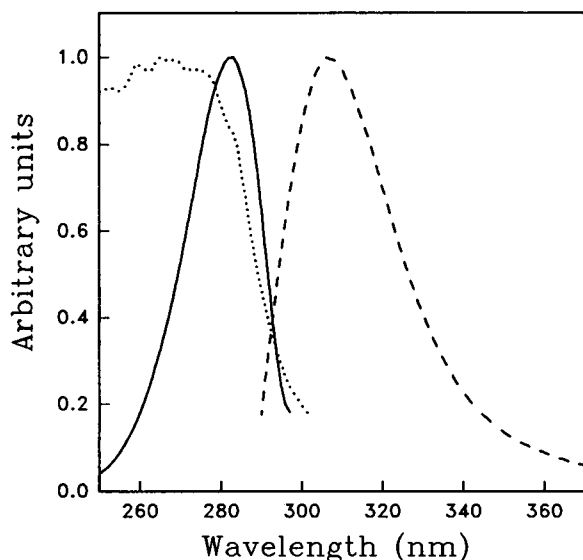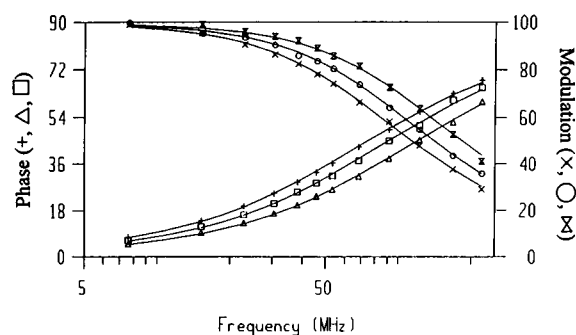

FIGURE 1 Ultraviolet absorption (...), corrected fluorescence excitation (–) and fluorescence emission (–) spectra of purified BSOD. Samples contained 60 μM BSOD in 10 mM Tris-Cl buffer, pH 7.6, 1 mM DTT. Absorption was measured in a Perkin-Elmer Lambda-5 spectrophotometer (1-nm bandpass). Fluorescence spectra were acquired as described in Materials and Methods. For the excitation spectrum, emission was fixed at 306 nm; for the emission spectrum excitation was at 283 nm.

TABLE 1 BSOD fluorescence lifetime data analysis[a]

Temp (°C)	Single Exponential		Double Exponential				Triple Exponential						
	τ	χ^2	τ_1	τ_2	f_1 (α_1)	χ^2	τ_1	τ_2	τ_3	f_1 $(\alpha 1)$	f_2 $(\alpha 2)$	f_3	χ^2
	ns		ns	ns		ns	ns	ns					
8	2.2	133	4.3	1.6	0.41 (0.21)	4.5	1.9	5.7	0.00	0.75 (0.90)	0.24 (0.10)	0.01	1.0
15	2.1	124	3.7	1.4	0.45 (0.24)	3.3	1.7	4.7	0.00	0.72 (0.88)	0.27 (0.12)	0.01	1.3
20	2.0	103	3.8	1.4	0.37 (0.18)	2.9	1.7	4.8	0.00	0.77 (0.91)	0.22 (0.09)	0.01	1.1
26	1.9	95	4.2	1.5	0.28 (0.12)	5.8	1.6	5.3	0.00	0.81 (0.94)	0.18 (0.06)	0.01	4.8
30	1.7	98	3.0	1.2	0.44 (0.24)	4.2	1.6	4.5	0.02	0.80 (0.93)	0.18 (0.07)	0.02	1.2
36	1.6	97	3.5	1.3	0.30 (0.14)	2.6	1.3	3.9	0.00	0.75 (0.90)	0.24 (0.10)	0.01	2.5
45	1.4	81	2.2	0.9	0.57 (0.35)	9.2	1.3	3.5	0.05	0.79 (0.93)	0.17 (0.07)	0.04	2.8
L-Tyr (20°C)[b]	3.3	1.4	–	–	–	–	–	–	–	–	–	–	–

[a] Different exponential decay models were fitted to phase-modulation lifetime data. In the double- or triple-exponential fit, f_i is the fractional fluorescence intensity associated with τ_i. The amplitudes (preexponential factors) for each lifetime component are also given between parenthesis. For the triple-exponential fit, amplitudes were calculated after subtracting the scatter component. χ^2 is the reduced chi-squared for the fits.
[b] L-tyrosine (60 μM) in 10 mM Tris-HCl buffer, pH 7.6, 25°C.

sampling of an underlying physical continuous distribution. In this case, information on the underlying distribution can be obtained by calculating the moments of the distribution defined by the exponential parameters. The center of the distribution can be approximated by calculating the first-order moment or weight-averaged lifetime ($<\tau> = \Sigma \ \tau_i f_i$). From the three-exponential fit, the width of the distribution can be approximated by the second-order moment (standard deviation) calculated as $\sigma = [\ \Sigma((<\tau> - \tau_i f_i)^2)/3]^{1/2}$. The calculated parameters using the three-exponential fit from Table 1 are shown as a function of temperature in Fig. 3. Increasing temperature produced continuous decreases in both the center and width of the reconstructed lifetime distribution. This is the same qualitative behavior that has been observed as a function of temperature for the fluorescence decay of proteins containing a single tryptophan residue (Alcala et al., 1987b; Ferreira, 1989; Rosato et al., 1990a). In the latter studies, the fluorescence decays were described utilizing continuous distributions of lifetime values, which prompted us to use distribution analysis with our data for BSOD.

Phase-modulation data for BSOD were fitted with continuous distributions of lifetime values of various analytical forms and shapes (Table 2). Symmetric Gaussian or uniform distribution, as well as skewed gamma distribution models gave poor fits to the data, as indicated by the high χ^2 values obtained (Table 2). Significant decreases in χ^2 were obtained with the Lorentzian distribution fits. Slightly lower χ^2 values (as compared to the Lorentzian fits) were obtained employing skewed Planck distribution fits. However, it is important to note that the Planck distribution employs three fitting parameters versus only two parameters with the other distributions tested. Thus, statistical evaluation was required to
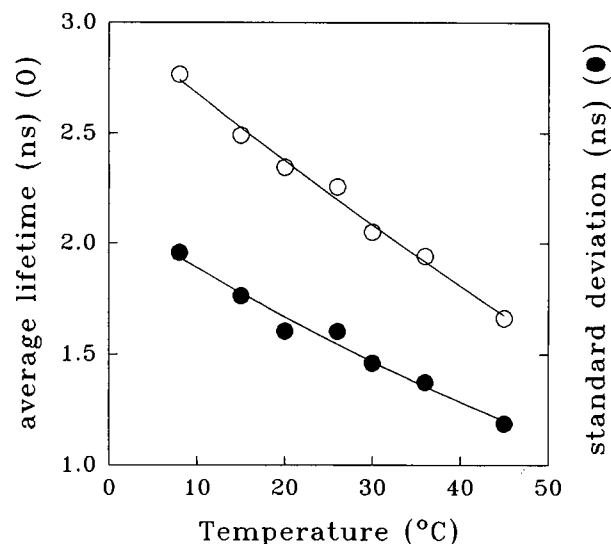

FIGURE 3 Temperature dependence of distribution parameters recovered from three-exponential analysis. Phase-modulation data were analyzed with a three-exponential decay model and the moments of the distribution sampled by the three-exponential parameters were calculated, as described in Results.

determine the significance of the decrease in χ^2 with the Planck distribution relative to the Lorentzian distribution fits. F-statistics analysis (Motulsky and Ransnas, 1987) indicated that the confidence levels for statistically significant decrease in χ^2 with the Planck fits ranged from 0.78 to only 0.89 for five out of seven temperatures tested, whereas no improvement in χ^2 was noted at the other two temperatures. Furthermore, significantly larger uncertainties in recovered parameters were obtained in rigorous error analysis (Beechem

TABLE 2   BSOD fluorescence lifetime data analysis[a]

Temp (°C)	Gaussian χ^2	Uniform χ^2	Gamma χ^2	Planck χ^2	Lorentzian		
					c	w	χ^2
8	13.6	7.7	24.3	3.1	2.33	1.0	4.5
15	10.8	5.2	19.1	2.2	2.14	0.9	3.1
20	12.8	6.5	14.6	2.0	2.00	0.8	3.7
26	18.4	12.5	17.3	5.0	1.90	0.7	8.1
30	10.0	5.2	14.3	3.2	1.76	0.7	2.5
36	15.5	9.0	16.1	2.3	1.65	0.6	6.1
45	15.8	8.8	14.6	7.5	1.45	0.6	4.0

[a] Continuous lifetime distributions of different analytical forms were fitted to phase-modulation lifetime data. The analytical expressions for Gaussian, uniform, Lorentzian, and Planck distributions are described in Alcala et al. (1987a), and for the gamma distribution in DiIorio et al. (1991). Symmetric Gaussian, uniform, and skewed gamma distribution models gave poor fits to the data, and for simplicity only χ^2 values are shown for these distributions. For the symmetric Lorentzian distribution model the center (c) and width (w) of the recovered distributions are shown in addition to χ^2 values. F-statistics analysis indicated that the slightly lower χ^2 values (as compared to the Lorentzian fits) obtained with the skewed Planck distribution were not statistically significant (see Results) because the Planck function contains one more fitting parameter, and for simplicity the parameters recovered in this distribution were also omitted from Table 2.

and Gratton, 1988) of the results of Planck fits relative to Lorentzian fits (not shown). Therefore, in light of the above statistical considerations, the Planck distribution was not employed further in the analysis of BSOD lifetime data. Fits of data with bimodal lifetime distributions (five fitting parameters) were also found not to be statistically significant.

It is also interesting to compare the results of the Lorentzian distribution fits with those obtained with two- or three-exponential models. For the two-exponential fits, F-statistics analysis indicated that the confidence levels for statistically significant decrease in χ^2 relative to Lorentzian fits ranged from 0.74 to only 0.88 for three out of seven temperatures tested, whereas no improvement was noted at the other four temperatures. For the three-exponential fits, statistically significant decreases in χ^2 relative to Lorentzian fits (confidence levels ranging from 0.92 to 0.98) were observed for five temperatures, whereas for the other two temperatures nonsignificant decreases were found. These findings, and the above discussed physical interpretation of the results of the three-exponential fits led us to conclude that the Lorentzian distribution fit gave a good description of the fluorescence decay of BSOD. It should be clear, however, that the real physical distribution is probably more complex than the Lorentzian.

Control measurements of the fluorescence decay of L-tyr in aqueous buffer indicated that the fluorescence decay was accurately described by a single-exponential in the temperature range from 10 to 50°C (Table 1; see also Fig. 5A, inset). Analysis of L-tyr data with a Lorentzian distribution showed that the Lorentzian collapsed to a single exponential decay. This rules out the possibility that the heterogeneity in the fluorescence decay of BSOD results from instrumental response, and suggests that the heterogeneity arises from interaction of the tyr residue with the protein matrix. At 20°C

a lifetime of 3.3 ns was observed for L-tyr (Table 1), which is in good agreement with literature values (Lakowicz et al., 1987). Lower χ^2 values were in general obtained in our fits of L-tyr data than of BSOD data. This suggests misweighting of errors in the analysis of BSOD data, which may be due to the existence of systematic errors in the measurements that are not accounted for in our estimate of experimental errors (see Materials and Methods). Systematic errors may originate from long-term drifts in stability of the laser light source or in the acquisition electronics. More importantly, the possible presence of small amounts of parasitic light in the measurements with BSOD (see above), and its absence in the measurements with L-tyr, may also contribute for the differences in χ^2.

The effect of temperature on the fluorescence lifetime distributions of BSOD is shown in Fig. 4. Increasing temperature promoted a significant shift in the center of the distribution (corresponding to the average fluorescence lifetime) to lower values and a decrease in the width of the distribution. Temperature effects on the lifetime distributions were reversible, indicating that no denaturation of BSOD occurred in the temperature range investigated.

The change in the center of the lifetime distribution of BSOD as a function of temperature is shown in Fig. 5A. The dependence of the center on temperature was analyzed in terms of an Arrhenius model for thermal quenching, as:

$$1/C(T) = k_1 + k_0 \exp(-E_a/RT), \quad (1)$$

where C is the center of the lifetime distributions, k_1 is the radiative decay rate, k_0 is the nonradiative thermal rate constant at infinite temperature, E_a is the activation energy, and R and T have their usual meanings. The inset in Fig. 5A shows Arrhenius plots for the temperature dependence of the center of the lifetime distribution in BSOD (closed circles), as well as for the lifetime of L-tyr in aqueous buffer under
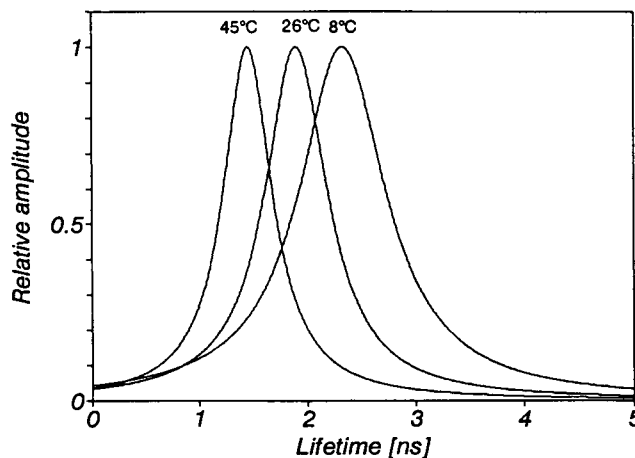

FIGURE 4 Fluorescence lifetime distributions in BSOD. Phase-modulation lifetime data were analyzed according to a unimodal Lorentzian lifetime distribution (Table 2). The distributions at 8, 25, and 45°C are shown. The curves are normalized for a relative amplitude of 1 at the center of the lifetime distribution.
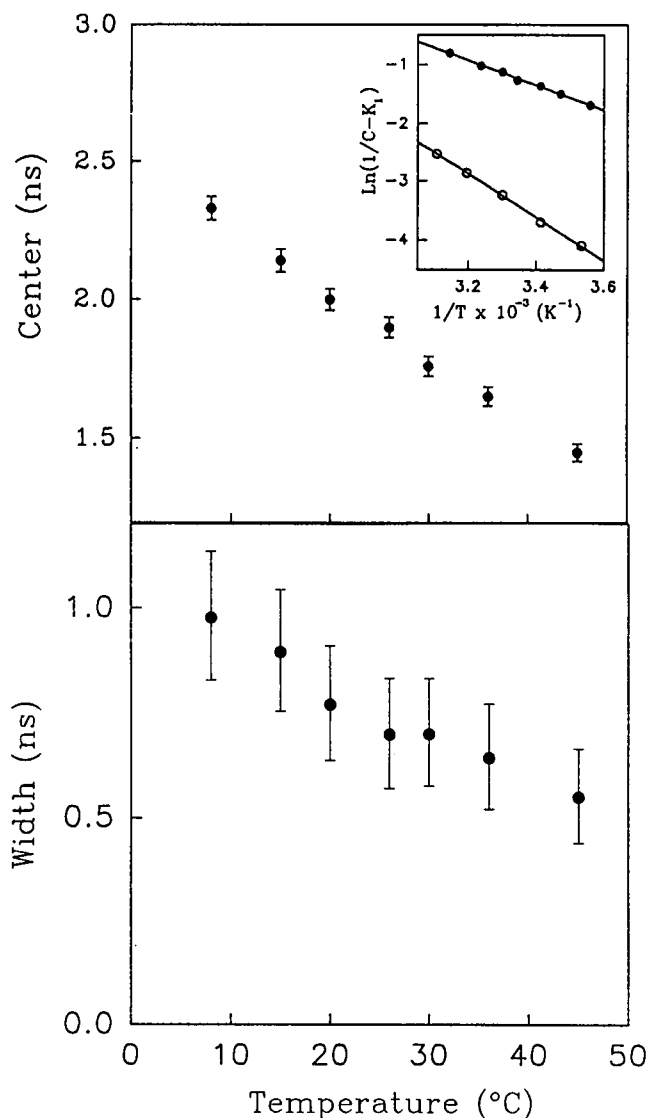
FIGURE 5 (A) Temperature dependence of the center of the lifetime distribution. Phase-modulation data for BSOD at temperatures ranging from 8 to 45°C were analyzed according to a Lorentzian lifetime distribution (Table 2) and the center of the distribution is shown as a function of temperature. Error bars in the figure represent confidence intervals encompassed by one standard deviation of the mean, obtained from χ^2-surface error analysis (Beechem and Gratton, 1988). Inset: Arrhenius plot (see Results) of BSOD lifetime data (●), yielding an activation energy, E_a, of 4.2 kcal/mol; for comparison, lifetime data for L-tyr as a function of temperature are also presented (○), yielding an E_a of 7.4 kcal/mol. Solid lines are nonlinear least-squares fits according to the Arrhenius model described in Results. (B) Temperature dependence of the width of the lifetime distribution.

identical conditions (*open circles*). Activation energies of 4.2 and 7.4 kcal/mol were found for BSOD and L-tyr, respectively.

The heterogeneity (width) of protein lifetime distributions has been related to the existence of conformational substates of the protein and to the rate of interconversion between them (Alcala et al., 1987 a–c; Gratton et al., 1988; Bismuto et al., 1988; Ferreira, 1989; Mei et al., 1992). We have therefore investigated the effects of different environmental conditions

on the width of the lifetime distribution of BSOD, as a probe of the conformational dynamics of this protein. Fig. 5 *B* shows that increasing temperature from 8 to 45°C produced a significant decrease in the width of the lifetime distribution of BSOD. The statistical significance of the decrease in width as a function of temperature was examined by performing a simultaneous fit (Beechem et al., 1991) of the datasets at different temperatures and linking the width between datasets, so that the width parameter was minimized for the value that best fit simultaneously to all datasets. This linked analysis yielded a global χ^2 of 6.5, as compared to a global χ^2 of 4.6 for the analysis with free-floating widths in all datasets. Taking into account the number of degrees of freedom for the two fits, F-statistics analysis of the difference in χ^2 between them indicated a confidence level of 0.994 for a statistically significant improvement in fit in the free analysis relative to the linked analysis.

The rate of interconversion between conformational substates in BSOD should also be dependent on the viscosity of the medium, which would be expected to change the height of the energy barriers between substates (Beece et al., 1980). Therefore, measurements of the fluorescence decay of BSOD at different viscosities should reflect changes in the dynamics of the protein matrix. Measurements were carried out by adding a fixed concentration of glycerol to the samples, and performing measurements at different temperatures. Thus, any possible effects of glycerol per se (Timasheff and Arakawa, 1989) on BSOD structure were constant in all datasets, allowing for evaluation of the effect of viscosity in a more straightforward manner. Fig. 6 shows the width of the lifetime distributions obtained at different temperatures in the presence of 80% (v/v) glycerol. The width was markedly
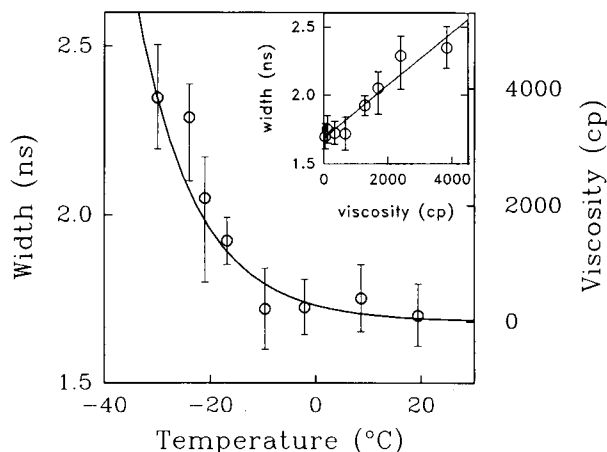

FIGURE 6 Effect of viscosity on the width of the lifetime distribution. Phase-modulation data acquired at different temperatures in the presence of 80% (v/v) glycerol were analyzed as Lorentzian lifetime distributions. Lorentzian fits yielded χ^2 values of 4.3, 1.4, 1.9, 1.0, 3.7, 1.4, 2.3, and 2.1, respectively, for data measured at −30, −24, −21, −17, −10, −2, 9, or 19°C. Error bars are as described in the legend to Fig. 5. The change in viscosity of the solution as a function of temperature is also shown (*solid line*, viscosity data from Miner (1953)). The inset shows a plot of the distribution width versus viscosity of the medium; the line through the points was obtained by linear regression.

dependent on the viscosity of the medium, as shown by the parallelism between the experimental data (*open circles*) and viscosity (*solid line* in Fig. 6). That the change in width observed in Fig. 6 is due to the increase in viscosity of the medium and not to a direct effect of temperature can be concluded from a comparison of the magnitudes of the two effects on the rate of interconversion between substates. The rate of interconversion is inversely proportional to viscosity and directly dependent on temperature through an Arrhenius term (Kramers, 1940). In the temperature range investigated in Fig. 6 viscosity changed by a factor of approximately 80 (Miner, 1953), whereas assuming an energy barrier of 1–4 kcal/mol the temperature term changes only by a factor between 1.4 and 4. Thus, we conclude that the viscosity effect is one to two orders of magnitude larger than the temperature effect.

Recent reports have shown that protein denaturation may lead to an increase in heterogeneity of the fluorescence decay, indicating a larger number of conformations in the unfolded protein relative to the native state (Bismuto et al., 1988; Mei et al., 1992). The fluorescence decay of BSOD was investigated in the presence of the denaturant GdHCl. Lifetime data obtained at increasing GdHCl concentrations were analyzed with the unimodal Lorentzian distribution model, which yielded good fits to the data up to 7 M GdHCl. Fig. 7 shows the behavior of the center and the width of the lifetime distribution as a function of GdHCl concentration. A sharp increase in width was observed between 4 and 6 M GdHCl (*open circles*). The center of the lifetime distribution (*closed circles*) was not significantly affected by denaturation of BSOD. Under identical conditions, no significant

changes were observed in the fluorescence emission spectrum of BSOD up to 7 M GdHCl (not shown). As a control, we have also measured the fluorescence decay of L-tyr in aqueous buffer in the absence or in the presence of 7 M GdHCl. No changes in the single-exponential lifetime of L-tyr were observed upon addition of 7 M GdHCl (data not shown).

The conformational dynamics of BSOD was further investigated by measuring directly the orientational mobility of tyr 108. Fluorescence anisotropy decay measurements were carried out at temperatures ranging from 10 to 40°C, and data were analyzed in terms of one or two rotational correlation times (Table 3). For the fits to anisotropy decay data, independent determination of the limiting anisotropy, r_0, of tyr at the excitation wavelength used (283 nm) was desired. Measurement of r_0 for Ltyr in aqueous solution containing 80% (v/v) glycerol at –21°C yielded a value of 0.285, which was in excellent agreement with the literature value of 0.29 ± 0.01 (Gryczynski et al., 1991). An identical r_0 of 0.285 was found for tyr 108 of BSOD under the same conditions, which excludes the possibility that energy transfer between tyr residues (one on each subunit of dimeric BSOD) causes depolarization of the fluorescence. Table 3 shows that very high χ^2 values were obtained in the fit of a single rotational correlation time to the anisotropy decay data, using $r_0 = 0.285$. If the value of r_0 was allowed to vary in the fit an improvement in χ^2 resulted, but the recovered r_0 value was 0.13 (Table 3), which was not compatible with the independently determined value of 0.285 for BSOD. Instead, very good fits to the data were obtained employing two discrete rotational correlation times and $r_0 = 0.285$ (Table 3). Both correlation times decreased with increasing temperature (Fig. 8), indicating faster motions at higher temperatures.

The temperature dependence of the long correlation time (ϕ_1, ranging from 9.1–4.7 ns from 10 to 40°C, respectively; Table 3) could be fit in terms of the Stokes-Einstein relationship, as:

$$\phi_1 = \eta V/RT, \qquad (2)$$

where η is the viscosity of the medium and V is the hydrated molar volume of the protein. The volume of the equivalent rotating sphere obtained from this fit (Fig. 8, *inset*) was 16,000 ml/mol, which corresponded to 50% of the volume (31,000 ml/mol) calculated, taking into account the molecular weight of dimeric BSOD and a hydration of 0.3 g of H_2O/g of protein (Cantor and Schimmel, 1980). The short correlation time (50–120 ps; Table 3) accounted for 62% (i.e., a preexponential factor of 0.175) of the fluorescence depolarization, and likely originated from local mobility of tyr 108.
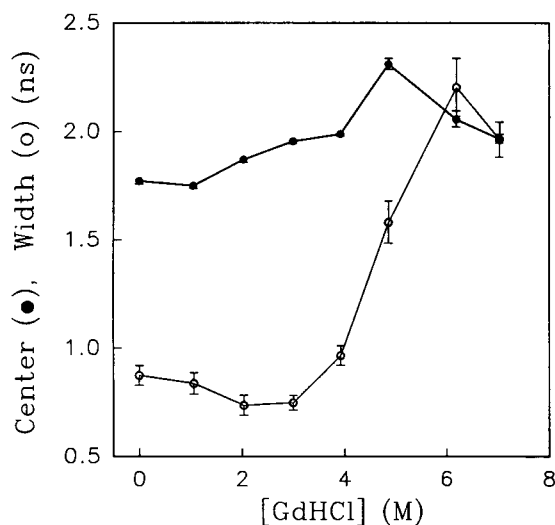

FIGURE 7 Effect of guanidine hydrochloride on the fluorescence decay of BSOD. Individual samples were incubated in the presence of the indicated concentrations of GdHCl for 20 h at 4°C, and phase-modulation measurements were carried out at 20°C. The figure shows the center (●) and width (○) of the unimodal Lorentzian lifetime distribution recovered at each concentration of GdHCl. The recovered χ^2 for the fits at 0, 1, 2, 3, 4, 5, 6, or 7 M GdHCl were, respectively, 1.4, 1.6, 1.7, 0.8, 0.8, 1.5, 5.3, and 2.3. Error bars are as described in the legend to Fig. 5.

DISCUSSION

A large number of studies have taken advantage of the high sensitivity of trp fluorescence to the physicochemical characteristics of the surrounding medium to probe protein conformation. Much less has been done using tyr fluorescence

TABLE 3   Fluorescence anisotropy decay data analysis

Temp (°C)	Single-Exp $(r_0 = 0.285)$[a]		Single-Exp $(r_0$ linked)[b]		Double-Exp[c] $(r_0 = 0.285)$		
	ϕ	χ^2	ϕ	χ^2	ϕ_1	ϕ_2	χ^2
	ns		ns		ns	ns	
10	0.9	538	5.3	7.5	9.1	0.12	2.5
15	0.8	501	4.6	5.3	7.5	0.09	1.2
20	0.7	444	4.1	11	6.5	0.09	1.6
25	0.7	405	3.8	7.3	5.9	0.08	2.7
30	0.6	378	3.6	6.6	5.5	0.08	1.1
35	0.6	342	3.3	7.1	4.8	0.07	1.5
40	0.5	343	3.1	5.9	4.7	0.05	1.5

[a] In this single-exponential fit r_0 was fixed at 0.285.

[b] In this single-exponential fit r_0 was allowed to vary, but was globally linked throughout the datasets at different temperatures; the minimized value of r_0 in this case was 0.13.

[c] In this fit the pre-exponential factors corresponding to each rotational correlation time were globally linked throughout the datasets at different temperatures; the recovered amplitudes in the global fit were 0.110 and 0.175 for ϕ_1 and ϕ_2, respectively. The limiting anisotropy, r_0, was fixed at 0.285.

in proteins lacking trp (for a comprehensive review on tyr fluorescence in proteins see Ross et al., 1992). This may be partly due to the lack of sensitivity of the Stokes shift of tyr to the polarity of the medium. However, tyr fluorescence in proteins can be quenched by a number of different mechanisms without appreciable change in the emission spectrum depending on the environment of the tyr residue, including its location relative to nearby quenching side chains (Ross et al., 1992). Therefore, measurements of the fluorescence quantum yield and, particularly, of the fluorescence decay of tyr residues may provide information on protein conformational dynamics, because motions of the protein matrix could affect the relative distances and/or orientation between the tyr and quenching groups.

Heterogeneity of the fluorescence decay of BSOD

Measurements of the fluorescence decay of BSOD under different conditions of temperature, viscosity, or presence of denaturant revealed a heterogeneous decay (Tables 1 and 2). Multi-exponential fluorescence decays have been described for a number of single-tyr proteins. Double- or triple-exponential decays have been reported, for example, for histone H1 (Libertini and Small, 1985), pike parvalbumin (Permyakov et al., 1985), calbindin (Rigler et al., 1990), lima bean trypsin inhibitor (Nordlund et al., 1986), Leu[5] enkephalin (Lakowicz et al., 1987), motilin (Backlund and Graslund, 1992), and oxytocin (Ross et al., 1986; Lakowicz et al., 1986, 1987). This is similar to the observations for a large number of single-trp proteins (Beechem and Brand, 1985). For single-trp proteins, the observation of multi- or nonexponential decays led to the introduction of continuous lifetime distributions as an alternative physical description of the fluorescence decay (Alcala et al., 1987 a–c; Gratton et al., 1989; Libertini and Small, 1989). Lifetime distributions have been used to describe conformational fluctuations of proteins during the excited-state lifetime of the trp residue (Alcala et al., 1987b; Gratton et al., 1988, 1989; Bismuto et al., 1988; Ferreira, 1989; Rosato et al., 1990 a, b; Mei et al., 1992). To

date, however, lifetime distributions had not been employed to describe the fluorescence decay of tyr residues in proteins. As discussed below, we believe that the lifetime distribution model was useful in providing a physical interpretation for the effects of environmental conditions on the conformations of BSOD.

An interesting question pertains to the origin of the nonexponential fluorescence decay of tyr in proteins. It should be noted that although L-tyr displays a single exponential lifetime, some tyr derivatives (e.g., N-acetyl-tyrosinamide) and model di- or tri-peptides containing tyr display biexponential decay kinetics (Laws et al., 1986; Lakowicz et al., 1987; Ross et al., 1992). This finding was explained in terms of ground-state heterogeneity of different rotamers resulting from rotation about the $C\alpha$-$C\beta$ bond of tyr (Gauduchon and Wahl, 1978; Laws et al., 1986). However, there is still controversy in this respect, because Gauduchon and Wahl (1978) noted, on the basis of NMR and fluorescence data, that the rotational rate about this bond should in fact be similar to the tyr lifetime. Furthermore, a recent molecular dynamics investigation of solvated tyr and a tyr-containing tripeptide has indicated fast rotational rates about the $C\alpha$-$C\beta$ bond relative to the lifetime of the fluorophore (Kungl, 1992). In addition, fluorescence anisotropy measurements indicate that in proteins tyrosine has a relatively large orientational mobility in the 10–100 ps time scale (see discussion below of tyr rotations in BSOD).

Temperature effects on the fluorescence decay of BSOD

Lifetime measurements at temperatures ranging from 8 to 45°C revealed that the fluorescence decay of BSOD was dependent on temperature (Tables 1 and 2). Increasing temperature decreased both the average lifetime and the heterogeneity of the decay (width of the lifetime distribution). Similar temperature effects have been described for the homologous protein, human SOD (Rosato et al., 1990b), and for whiting parvalbumin (Ferreira, 1989). In those studies, the
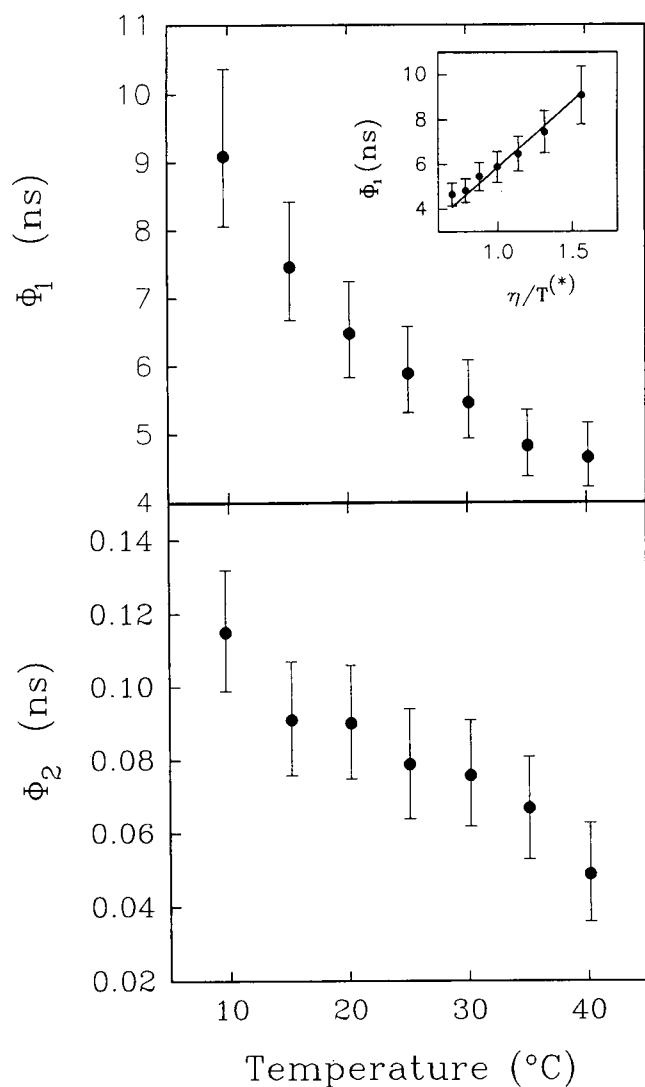
FIGURE 8   Effect of temperature on the rotational correlation times of BSOD. Fluorescence anisotropy decay data were acquired at different temperatures and analyzed in terms of two rotational correlation times. (Panel A) Long rotational correlation time as a function of temperature. The inset shows a fit of the long correlation time to the rotational diffusion equation described in Results; η/T ratio in the abscissa is normalized to the value at 25°C. (Panel B) Short rotational correlation time as a function of temperature.

behavior of the width of the lifetime distribution as a function of temperature has been explained in terms of a temperature effect on the rates of interconversion between conformational substates in the proteins. Increasing temperature should lead to increased interconversion rates. This in turn should lead to an increased averaging of the different environments sampled by the fluorophore during the excited-state, and consequently to a narrower lifetime distribution (Ferreira, 1989). Lowering temperature, on the other hand, should decrease interconversion rates and trap the protein in a large number of substates, leading to a broader lifetime distribution. This was the behavior observed with BSOD (Figs. 3–5), suggesting that the width of the lifetime distri-

bution does reflect the rate of interconversion between substates in this protein.

Interpretation of the effect of temperature on the center of the distribution is less clear. It should be noted, however, that a simple mechanism of thermal quenching of tyr fluorescence was not adequate to explain the data for BSOD. This was apparent from a comparison of the Arrhenius thermal quenching analysis for BSOD and for L-tyr in buffer (Fig. 5 A, inset). Whereas an activation energy of 7.4 kcal/mol was found for thermal quenching of L-tyr fluorescence, an activation energy of 4.2 kcal/mol was found for BSOD. The lower activation energy of the average lifetime of tyr 108 in BSOD relative to L-tyr in buffer is likely due to a combined effect of thermal quenching and protein motions on the fluorescence decay.

Effect of viscosity on the heterogeneity of the decay

The dynamic nature of protein structures has been related to the existence of a hierarchy of conformational substates (Frauenfelder and Gratton, 1986). The effect of solvent viscosity on protein dynamics has been investigated by Beece and co-workers (1980). These authors showed that increasing viscosity decreased the interconversion between substates. This model implies that protein motions and solvent conditions are closely coupled (the rate of interconversion between substates is proportional to $1/\eta$). Therefore, if the dynamic interpretation we propose for the width of the lifetime distribution of BSOD is valid, we would expect to observe broader distributions at high solvent viscosity. In fact, the width of the lifetime distribution closely followed the increase in viscosity of the medium (Fig. 6). An additional point that should be considered is the possibility of direct effects of glycerol on the fluorescence of the solvent-exposed tyrosine residue in BSOD. As previously noted (see Materials and Methods), we have carried out the lifetime measurements by collecting the fluorescence emission through a long-pass filter. Thus, any effects due to solvent dipolar relaxation in the presence of glycerol are not likely to influence our measurements. In addition, we have measured the fluorescence decay of L-tyr in the presence of 80% glycerol. Our results (Ferreira and Gratton, unpublished results) show that, whereas L-tyr in aqueous buffer has a single exponential lifetime ($\tau = 3.3$ ns), addition of 80% glycerol causes the fluorescence decay to become bi-exponential ($\tau_1 = 4.3$ ns; $\tau_2 = 1.8$ ns; $f_1 = 0.80$). This is similar to what we have observed for tryptophan in the presence of glycerol (Silva and Gratton, unpublished observations), and suggests that in the highly viscous glycerol solution different conformations of the tyrosine molecule (corresponding to different lifetimes) may be observed.

Unfolding of BSOD

Lifetime measurements of BSOD were carried out in the presence of the denaturant GdHCl. Early studies have shown

that holo-BSOD is remarkably stable, and high concentrations of GdHCl were required to produce significant unfolding (Forman and Fridovich, 1973). The lifetime distribution width was found to be markedly dependent on unfolding of the protein, with a sharp increase in width occurring between 4 and 6 M GdHCl (midpoint transition at ~5 M GdHCl, Fig. 7). The increase in distribution width indicated an increase in the number of conformations of the polypeptide chain in the denatured state relative to the more compact, native state. It is noteworthy that a decrease in distribution width would be expected if the polypeptide chain was completely unfolded by GdHCl (i.e., in a random-coil state): in this case the tyr residue would be fully exposed to the solvent and free from contacts with proximal quenching groups in the protein. Thus, our data indicate that some degree of structure is maintained in BSOD even at 7 M GdHCl. This result is in line with previous reports on the thermal denaturation of myoglobin monitored by time-resolved fluorescence (Bismuto et al., 1988), which also indicated an increase in conformational heterogeneity in the unfolded state.

Rotations in BSOD

Analysis of anisotropy decay data for BSOD enabled resolution of two rotational correlation times (Table 3), indicating that, in addition to overall rotation of the protein molecule, information on local mobility of the fluorophore could be obtained from such measurements (Munro et al., 1979; Ferreira, 1989; Mei et al., 1992). The fast correlation time (50–120 ps; Fig. 8 B) likely corresponded to rotational motions of the tyr sidechain. This fast rotation was responsible for about 62% of the fluorescence depolarization, suggesting large amplitude motions of tyr 108. The angular displacement of tyr 108 corresponding to this rapid depolarization can be obtained from:

$$r/r_0 = 1/2(3 \cos^2\theta - 1), \tag{3}$$

where θ is the semi-angle through which the group is free to rotate, and r/r_0 is the fractional anisotropy remaining after depolarization due to the fast rotation. Alternatively, a "wobbling in a cone" model (Kinosita et al., 1977) may be used to calculate the cone angle θ_m in which the tyr rotates:

$$r/r_0 = [1/2(\cos \theta_m(1 + \cos \theta_m))]^2. \tag{4}$$

Angles of 30 or 32° were calculated from Eqs. 3 or 4, respectively, indicating that rather large angular displacements are experienced by tyr 108 during the excited state.

The long correlation time (Fig. 8 A) was 50% of the value calculated for rotation of the BSOD dimer. There is considerable evidence in the literature regarding the very high stability of holo-BSOD (Forman and Fridovich, 1973; Lepock et al., 1985; Roe et al., 1988; McRee et al., 1990; Lepock et al., 1990; Rigo et al., 1978; Malinowski and Fridovich, 1979). These studies indicate that temperatures in excess of 70–80°C are required to produce inactivation and denaturation of BSOD, and that even under conditions such as incubation with 4% SDS at 37°C for 36–48 h or in the presence

of 8 M urea for 72 h the dimeric structure of BSOD is still maintained (Rigo et al., 1978; Malinowski and Fridovich, 1979). The subunits of BSOD are held together by strong noncovalent interactions, and attempts at monomerization of the enzyme revealed that monomers could only be obtained under strongly denaturing conditions resulting from a combination of (1) metal ion removal, (2) denaturing agents, and (3) extremes of pH or temperature (Valentine and Pantoliano, 1981). Thus, under the conditions employed in the present studies (temperatures ranging from 8 to 45°C, and physiologic pH), holo-BSOD remains in its native dimeric state. These considerations and the linearity of the Stokes-Einstein plot shown in the inset of Fig. 8 indicate that the decrease in the long correlation time with increasing temperature (Fig. 8) is not due to subunit dissociation or unfolding, and suggest that this correlation time reflected segmental or domain motions of the polypeptide chain. We have also tried to analyze the anisotropy decay data with a model employing a fixed long rotational correlation time, corresponding to the expected rotational correlation time for dimeric BSOD (calculated from the molecular weight of the protein and assuming a hydration of 30%). In this fit, the recovered amplitude for this long correlation time was zero throughout the temperature range investigated (not shown), indicating that no further improvement was achieved by using this model instead of the bi-exponential model shown in Table 3. Thus, our data do not enable the determination of the overall rotation of the BSOD dimer, which is probably because most of the anisotropy decay is in fact due to very fast, local motions of the tyrosine ring. In addition, one should consider the short lifetime of the tyrosine fluorescence in BSOD (~2 ns), which renders the fluorescence decay little sensitive to relatively long-lived motions as the overall rotation of the dimer.

It is interesting to consider the time scale of the protein motions that could be expected to affect the fluorescence decay of BSOD. With an excited-state lifetime of 2 ns at 20°C (Table 2), fast picosecond local motions should produce an effective averaging of the different environments sampled by tyr 108 in its excited state. Thus, a homogeneous decay corresponding to the time-averaged lifetime in the different environments should result. Because a heterogeneous decay was observed, other motions must play determinant roles in this process. Overall rotation of the protein occurs in a slower time scale relative to the fluorescence decay, and would also not be expected to produce any heterogeneity in the decay. It appears likely that mobility of the protein matrix surrounding tyr 108 are the relevant motions that lead to heterogeneous fluorescence decay.

Similarities with human SOD

Comparison between the present results and those previously described with the single-trp human SOD (Rosato et al., 1990; Mei et al., 1992) shows significant qualitative similarities between these studies: 1) for both BSOD and human SOD the fluorescence decay was heterogeneous, despite the fact that a single fluorophore is present in either protein;

2) for both BSOD and human SOD the width of the lifetime distribution was significantly decreased with increasing temperatures; 3) for both proteins the center of the lifetime distribution became shorter at increasing temperatures, an effect that did not appear related to thermal quenching of the emission; and 4) for both proteins, unfolding by GdHCl caused a significant increase in the width of the lifetime distributions. Although quantitatively these effects were not identical for BSOD or human SOD given the different photophysical properties of trp and tyr, these results indicate that the dynamic qualitative behavior of the two homologous proteins is similar, regardless of whether trp or tyr are used as the intrinsic probe. The only qualitative difference we have observed between our results with BSOD and human SOD are related to the effect of unfolding on the average lifetime: whereas for human SOD an increase in lifetime upon unfolding was reported, the average lifetime of BSOD was not much affected by addition of GdHCl. This difference may be explained by a decrease of the quenching of the fluorescence of trp 32 in human SOD by neighboring aminoacid residues (such as asn 19, lys 30, or lys 3, which are in close contact with the indole ring in the crystal structure of human SOD; Parge et al., 1992) upon unfolding. Because trp 32 in human SOD and tyr 108 in BSOD are located in different regions of the protein quenching by neighboring aminoacid residues can be expected to be different for the two proteins. In conclusion, the similarities between the results with the two SODs indicate that the dynamic information conveyed by the fluorescence emission does not depend on the specific photophysics or position of the fluorophore. Rather, both fluorophores can be effectively used as probes of dynamic events of the protein matrix. We believe that, as in the case of trp-containing proteins, investigation of the fluorescence decay of tyr-containing proteins provides useful information on the conformational dynamics in these proteins.

REFERENCES

Alcala, J. R., E. Gratton, and F. G. Prendergast. 1987a. Resolvability of fluorescence lifetime distributions using phase fluorometry. *Biophys. J.* 51:587–596.

Alcala, J. R., E. Gratton, and F. G. Prendergast. 1987b. Fluorescence lifetime distributions in proteins. *Biophys. J.* 51:597–604.

Alcala, J. R., E. Gratton, and F. G. Prendergast. 1987c. Interpretation of fluorescence decays in proteins using continuous lifetime distributions. *Biophys. J.* 51:925–936.

Backlund, B.-M., and A. Graslund. 1992. Structure and dynamics of motilin. Time-resolved fluorescence of peptide hormone with single tyrosine residue. *Biophys. Chem.* 45:17–25.

Bannister, J. V., and W. H. Bannister. 1984. Isolation and characterization of superoxide dismutase. *Methods Enzymol.* 105:88–93.

Bannister, J., W. Bannister, and E. Wood. 1971. Bovine erythrocyte cuprozinc protein. 1. Isolation and general characterization. *Eur. J. Biochem.* 18:178–186.

Beece, D., L. Eisenstein, H. Frauenfelder, D. Good, M. C. Marden, L. Reinisch, A. H. Reynolds, L. B. Sorensen, and K. T. Yue. 1980. Solvent viscosity and protein dynamics. *Biochemistry.* 19:5147–5157.

Beechem, J. M., and L. Brand. 1985. Time-resolved fluorescence of proteins. *Ann. Rev. Biochem.* 54:43–71.

Beechem, J. M., and E. Gratton. 1988. Fluorescence spectroscopy data analysis environment: a second generation global analysis program. *SPIE (Time-resolved laser spectroscopy in biochemistry).* 909:70–81.

Beechem, J. M., E. Gratton, M. Ameloot, J. R. Knutson, and L. Brand. 1991. The global analysis of fluorescence intensity and anisotropy decay data: second generation theory and programs. *In* Topics in Fluorescence Spectroscopy. Vol. 2, Principles. J. R. Lakowicz, editor. Plenum Press, New York. 241–305.

Bismuto, E., E. Gratton, and G. Irace. 1988. Effect of unfolding on the tryptophanyl fluorescence lifetime distribution in apomyoglobin. *Biochemistry.* 27:2132–2136.

Cantor, C. R., and P. R. Schimmel. 1980. Biophysical Chemistry, vol 2. Freeman and Co., San Francisco, CA. 550–555.

Careri, G., P. Fasella, and E. Gratton. 1979. Enzyme dynamics: the statistical physics approach. *Ann. Rev. Biophys. Bioeng.* 8:69–97.

Deng, H.-X., A. Hentati, J. A. Tainer, Z. Iqbal, A. Cayabyab, W.-Y. Hung, E. D. Getzoff, P. Hu, B. Herzfeldt, R. P. Roos, C. Warner, G. Deng, E. Soriano, C. Smyth, H. E. Parge, A. Ahmed, A. D. Roses, R. A. Hallewell, M. A. Pericak-Vance, and T. Siddique. 1993. Amyotrophic lateral sclerosis and structural defects in Cu, Zn superoxide dismutase. *Science.* 261:1047–1051.

DiIorio, E. E., V. R. Hiltpold, D. Filipovic, K. H. Winterhalter, E. Gratton, E. Vitrano, A. Cupane, M. Leone, and L. Cordone. 1991. Protein dynamics. Comparative investigation on heme-proteins with different physiological roles. *Biophys. J.* 59:742–754.

Ferreira, S. T. 1989. Fluorescence studies of the conformational dynamics of parvalbumin in solution: lifetime and rotational motions of the single tryptophan residue. *Biochemistry.* 28:10066–10072.

Ferreira, S. T., and E. Gratton. 1990. Hydration and protein substates: fluorescence of proteins in reverse micelles. *J. Mol. Liq.* 43:253–272.

Forman, H. J., and I. Fridovich. 1973. On the stability of bovine superoxide dismutase: the effects of metals. *J. Biol. Chem.* 248:2645–2649.

Frauenfelder, H., and E. Gratton. 1986. Protein dynamics and hydration. *Methods Enzymol.* 127:207–216.

Frauenfelder, H., F. Parak, and R. D. Young. 1988. Conformational substates in proteins. *Ann. Rev. Biophys. Biophys. Chem.* 17:451–479.

Gauduchon, P., and P. Wahl. 1978. Pulse fluorimetry of tyrosyl peptides. *Biophys. Chem.* 8:87–104.

Gratton, E., N. Silva, and S. T. Ferreira. 1988. Fluorescence of tryptophan and protein dynamics. *In* Biological and Artificial Intelligence Systems. E. Clementi and S. Chin, editors. ESCOM Science Publishers, Leiden, The Netherlands. 49–56.

Gratton, E., J. R. Alcala, and F. G. Prendergast. 1989. Protein dynamics: fluorescence lifetime distributions. *In* Fluorescent Biomolecules. D. M. Jameson and G. Reinhart, editors. Plenum Press, New York. pp. 17–32.

Gryczynski, I., R. F. Steiner, and J. R. Lakowicz. 1991. Intensity and anisotropy decays of the tyrosine calmodulin proteolytic fragments, as studied by GHz frequency-domain fluorescence. *Biophys. Chem.* 39:69–78.

Gurd, F. R. N., and T. M. Rothgeb. 1979. Motions in proteins. *Adv. Prot. Chem.* 33:73–165.

Karplus, M., and J. A. McCammon. 1981. The internal dynamics of globular proteins. *CRC Crit. Rev. Biochem.* 9:293–349.

Kinosita, K., S. Kawato, and A. Ikegami. 1977. A theory of fluorescence polarization decay in membranes. *Biophys. J.* 20:289–305.

Kramers, H. A. 1940. Brownian motion in a field of force and the diffusion model of chemical reactions. *Physica (Amsterdan).* 7:284–304.

Kungl, A. J. 1992. Rotamer interconversion and its influence on the fluorescence decay of tyrosine: a molecular dynamics study. *Biophys. Chem.* 45:41–50.

Lakowicz, J. R., G. Laczko, and I. Gryczynski. 1986. Picosecond resolution of oxytocin tyrosyl fluorescence by 2 GHz frequency-domain fluorometry. *Biophys. Chem.* 24:97–100.

Lakowicz, J. R., G. Laczko, and I. Gryczynski. 1987. Picosecond resolution of tyrosine fluorescence and anisotropy decays by 2-GHz frequency-domain fluorometry. *Biochemistry.* 26:82–90.

Laws, W. R., J. B. A. Ross, H. R. Wyssbrod, J. M. Beechem, L. Brand, and J. C. Sutherland. 1986. Time-resolved fluorescence and ^{1}H NMR studies of tyrosine and tyrosine analogues: correlation of NMR-determined rotamer populations and fluorescence decay kinetics. *Biochemistry.* 25:599–607.

Lepock, J. R., L. D. Arnold, B. H. Torrie, B. Andrews, and J. Kruuv. 1985. Structural analyses of various Cu^{2+}, Zn^{2+}-superoxide dismutases by differential scanning calorimetry and Raman spectroscopy. *Arch. Biochem. Biophys.* 241:243–251.

Lepock, J. R., H. E. Frey, and R. A. Hallewell. 1990. Contribution of conformational stability and reversibility of unfolding to the increased thermostability of human and bovine superoxide dismutase mutated at free cysteines. *J. Biol. Chem.* 265:21612–21618.

Libertini, L. J. and E. W. Small. 1985. The intrinsic fluorescence of histone H1. Steady-state and fluorescence decay studies reveal heterogeneous emission. *Biophys. J.* 47:765–772.

Libertini, L. J., and E. W. Small. 1989. Application of method of moments analysis to fluorescence decay lifetime distributions. *Biophys. Chem.* 34:269–282.

Malinowski, D. P., and I. Fridovich. 1979. Subunit association and side-chain reactivities of bovine erythrocyte superoxide dismutase in denaturing solvents. *Biochemistry.* 18:5055–5060.

McNamara, J. O., and I. Fridovich. 1993. Did radicals strike Lou Gherig? *Nature.* 362:20–21.

McRee, D. E., S. M. Redford, E. D. Getzoff, J. R. Lepock, R. A. Hallewell, and J. A. Tainer. 1990. Changes in crystallographic structure and thermostability of a Cu, Zn superoxide dismutase mutant resulting from the removal of a buried cysteine. *J. Biol. Chem.* 265:14234–14241.

Mei, G., N. Rosato, N. Silva, Jr., R. Rusch, E. Gratton, I. Savini, and A. Finazzi-Agro. 1992. Denaturation of human Cu/Zn superoxide dismutase by guanidine hydrochloride: a dynamic fluorescence study. *Biochemistry.* 31:7224–7230.

Miner, C. S. 1953. Glycerol. Reinhold Publ. Corp., New York. pp. 278–283.

Motulsky, H. J., and L. A. Ransnas. 1987. Fitting curves to data using nonlinear regression: a practical and nonmathematical review. *FASEB J.* 1:365–374.

Munro, I., I. Pecht, and L. Stryer. 1979. Subnanosecond motions of tryptophan residues in proteins. *Proc. Natl. Acad. Sci. USA.* 76:56–60.

Nordlund, T. M., X.-Y. Liu, and J. H. Sommer. 1986. Fluorescence polarization decay of tyrosine in lima bean trypsin inhibitor. *Proc. Natl. Acad. Sci. USA.* 83:8977–8981.

Paoletti, F., and A. Mocali. 1990. Determination of superoxide dismutase activity by purely chamical system based on NAD(P)H oxidation. *Methods Enzymol.* 186:209–220.

Parge, H. E., R. A. Hallewell, and J. A. Tainer. 1992. Atomic structures of wild-type and thermostable mutant recombinant human Cu, Zn superoxide dismutase. *Proc. Natl. Acad. Sci. USA.* 89:6109–6113.

Permyakov, E. A., A. V. Ostrovsky, E. A. Burstein, P. G. Pleshanov, and C. Gerday. 1985. Parvalbumin conformers revealed by steady-state and time-resolved fluorescence spectroscopy. *Arch. Biochem. Biophys.* 240:781–791.

Rigler, R., J. Roslund, and S. Forsen. 1990. Side chain mobility in bovine calbindin D_{9k}. *Eur. J. Biochem.* 118:541–545.

Rigo, A., F. Marmocchi, D. Cocco, P. Viglino and G. Rotilio. 1978. On the quaternary structure of copper-zinc superoxide dismutases. Reversible dissociation into protomers of the isozyme I from wheat germ. *Biochemistry.* 17:534–537.

Roe, J. A., A. Butler, D. M. Scholler, J. S. Valentine, L. Marky, and K. J. Breslauer. 1988. Differential scanning calorimetry of Cu, Zn superoxide dismutase, the apoprotein, and its zinc-substituted derivatives. *Biochemistry.* 27:950–958.

Rosato, N., E. Gratton, G. Mei, and A. Finazzi-Agro. 1990a. Fluorescence lifetime distributions in human superoxide dismutase. Effects of temperature and denaturation. *Biophys. J.* 58:817–822.

Rosato, N., G. Mei, E. Gratton, J. V. Bannister, W. H. Bannister, and A. Finazzi-Agro. 1990b. A time-resolved fluorescence study of human copper-zinc superoxide dismutase. *Biophys. Chem.* 36:41–46.

Rosen, D. R., T. Siddique, D. Patterson, D. A. Figlewicz, P. Sapp, A. Hentati, D. Donaldson, J. Goto, J. P. O'Regan, H.-X. Deng, Z. Rahmani, A. Krizus, D. McKeena-Yasek, A. Cayabyab, S. Gaston, R. Berger, R. E. Tanzi, J. J. Halperin, B. Herzfeldt, R. VandenBergh, W.-Y. Hung, T. Bird, G. Deng, D. W. Mulder, C. Smyth, N. G. Laing, E. Soriano, M. Pericak-Vance, J. Haines, G. A. Rouleau, J. S. Gusella, H. R. Horvitz, and R. H. Brown. 1993. Mutations in Cu/Zn superoxide dismutase gene are associated with familial amyotrophic lateral sclerosis. *Nature.* 362:59–62.

Ross, J. B. A., W. R. Laws, A. Buku, J. C. Sutherland, and H. R. Wyssbrod. 1986. Time-resolved fluorescence and ^{1}H NMR studies of tyrosyl residues in oxytocin and small peptides: correlation of NMR-determined conformations of tyrosyl residues and fluorescence decay kinetics. *Biochemistry.* 25:607–612.

Ross, J. B. A., W. R. Laws, K. W. Rousslang, and H. R. Wyssbrod. 1992. Tyrosine fluorescence and phosphorescence from proteins and polypeptides. *In* Topics in fluorescence spectroscopy. Vol. 3. Biochemical applications. J. R. Lakowicz, editor. Plenum Press, New York. pp. 1–63.

Rusting, R. L. 1992. Why do we age? *Scientific American.* December 1992:131–141.

Tainer, J. A., E. D. Getzoff, K. M. Beem, J. S. Richardson, and D. C. J. Richardson. 1982. Determination and analysis of the 2 A structure of copper, zinc superoxide dismutase. *J. Mol. Biol.* 160:181–217.

Timasheff, S. N. and T. Arakawa. 1989. Stabilization of protein structure by solvents. *In* Protein Structure and Function: A Practical Approach. T. E. Creighton, editor. IRL Press, Oxford. pp. 331–345.

Valentine, J. S., and M. W. Pantoliano. 1981. Protein-metal ion interactions in cuprozinc protein (superoxide dismutase). A major intracellular repository for copper and zinc in the eukaryotic cell. *In* Copper Proteins. T. G. Spiro, editor. John Willey & Sons, New York. pp. 291–358.

Weber, G. 1977. Theory of differential phase fluorometry: detection of anisotropic molecular rotations. *J. Chem. Phys.* 66:4081–4091.

Wuthrich, K. 1976. Nuclear Magnetic Resonance in Biological Research - Peptides and Proteins. North-Holland, Amsterdam.

Zweier, J. L., J. T. Flaherty, and M. L. Weisfeldt. 1987. Direct measurement of free radical generation following reperfusion of ischemic myocardium. *Proc. Natl. Acad. Sci. USA.* 84:1404–1407.